Extended Conformation of Mammalian Translation Elongation Factor 1A in Solution[†]

T. V. Budkevich,[‡] A. A. Timchenko,[§] E. I. Tiktopulo,[§] B. S. Negrutskii,[‡] V. F. Shalak,[‡] Z. M. Petrushenko,[‡] V. L. Aksenov,[∥] R. Willumeit,[⊥] J. Kohlbrecher,[#] I. N. Serdyuk,[§] and A. V. El'skaya*,[‡]

Institute of Molecular Biology and Genetics, National Academy of Sciences, 150 Zabolotnogo Street, Kiev, 03143 Ukraine, Institute of Protein Research, Russian Academy of Sciences, Pushchino, Russia, Neutron Physics Laboratory, JINR, Dubna, Russia, GKSS Research Center, Geesthacht, Germany, and Paul Scherrer Institute, Villingen, Switzerland

Received July 23, 2002; Revised Manuscript Received October 22, 2002

ABSTRACT: The conformation of mammalian elongation factor eEF1A in solution was examined by the small angle neutron scattering and scanning microcalorimetry. We have found that in contrast to the bacterial analogue the eEF1A molecule has no fixed rigid structure in solution. The radius of gyration of the eEF1A molecule (5.2 nm) is much greater than that of prokaryotic EF1A. The specific heat of denaturation is considerably lower for eEF1A than for EF1A, suggesting that the eEF1A conformation is significantly more disordered. Despite its flexible conformation, eEF1A is found to be highly active in different functional tests. According to the neutron scattering data, eEF1A becomes much more compact in the complex with uncharged tRNA. The absence of a rigid structure and the possibility of large conformational change upon interaction with a partner molecule could be important for eEF1A functioning in channeled protein synthesis and/or for the well-known capability of the protein to interact with different ligands besides the translational components.

The eukaryotic translation elongation factor eEF1A[1] (formerly EF-1α) is a functional analogue of bacterial factor EF1A (formerly EF-Tu). The function of EF1A in prokaryotic cells is well studied. EF1A·GTP delivers the elongator aminoacyl-tRNA to the ribosome and promotes the accurate interaction of the tRNA anticodon with the codon of mRNA located at the ribosomal A-site. Following the codon−anticodon recognition, hydrolysis of GTP in the complex with EF1A takes place. As a result, the factor affinity for aminoacyl-tRNA and ribosome is lost. EF1A·GDP leaves the ribosome, and after the GDP/GTP exchange catalyzed by special factor EF1B (formerly EF-Ts), the protein can participate in the next elongation cycle.

Though the basic principles of the eEF1A functioning are similar to those of EF1A, there are some differences in the action of prokaryotic and eukaryotic proteins (*1*). One of the reasons may be the compartmentalization of the translation apparatus (*2*) serving as a structural basis for tRNA/aminoacyl-tRNA channeling during protein synthesis in mammalian cells (*3*). No indication of compartmentalization and channeling was observed in prokaryotic protein synthesis.

The channeling or vectorial transfer of tRNA/aminoacyl-tRNA means its transportation from the site of synthesis (aminoacyl-tRNA synthetase) to the site of utilization (ribosome) in such a way that aminoacyl-tRNA is never free and always remains bound to some protein(s) or ribosome (*4*). One of the noncanonical complexes thought to mediate the channeling of tRNA in mammalian cells is the [eEF1A·GDP·deacylated tRNA] complex (*5*). This complex was assumed to appear due to the acceptance of deacylated tRNA from the E-site of 80S ribosome by eEF1A·GDP (*1*). The putative function of this complex is to deliver tRNA from the ribosomal exit site to the aminoacyl-tRNA synthetase for subsequent recharging (*1*). The nonrandom, specific character of [eEF1A·GDP·tRNA] complex formation demonstrated by nuclease and chemical modification footprinting assay revealed a similarity of tRNA and aminoacyl-tRNA sites involved into the interaction with eEF1A·GDP and EF1A·GDPPNP, respectively (*5*, *6*).

Structural studies on EF1A involved in the various complexes with GDP or GTP/GDPPNP, aminoacyl-tRNA, and the exchange factor EF1B have provided an almost complete understanding of the molecular details of the EF1A functioning beyond the ribosome (*6−11*). Factor EF1A from *Escherichia coli* has the molecular mass of 43.15 kDa (*12*). The crystal structure of the protein complexed with GDP is known for trypsin-modified and native EF1A. The trypsin-modified EF1A molecule (*13*) consists of three distinct globular domains, connected by flexible interconnecting peptides, like beads on a string. The three domains form a flattened triangular shape of 7.5 nm by 5.0 nm by 3.0 nm. The theoretical radius of gyration calculated for such three-axis ellipsoid is 2.124 nm. The native EF1A·GDP molecule (*11*) has overall dimensions of 5.7 nm by 5.1 nm by 7.8 nm.

The theoretical radius of gyration calculated for such three-axis ellipsoid is 2.347 nm; the theoretical radius of gyration calculated with the CRYSOL program is 2.354 nm (*14*). According to the crystallographic data domain I (nucleotide-binding domain) is connected with domain II by a 1.6 nm long peptide. Domain III is connected with domain I by a short extended stretch of the polypeptide (*11*).

The solution structure of EF1A from *E. coli* was studied by small-angle neutron scattering using the procedure of triple isotopic substitution, and the radius of gyration was found equal to 2.39 nm (*15*). It should be mentioned that in the absence of GDP EF1A from *E. coli* is not stable; it is inactivated at 40 °C, but the thermal stability is strongly increased upon the addition of GDP (*16*). The rate of hydrogen/deuterium exchange for the free EF1A from *E. coli* at all pH values and temperatures used is higher than that for the GTP-bound or GDP-bound EF1A (*16*).

The crystal structures are also known for EF1A·GTP from *Thermus aquaticus* (*7*) and *Thermus thermophilus* (*8*). Molecular masses are 45.3 kDa (*17*) and 44.8 kDa (*18*), respectively. The polypeptide chain is folded into three domains, the overall structure of which is very close to that of EF1A·GDP from *E. coli.* The theoretical radius of gyration calculated with the CRYSOL program for EF1A·GTP from *T. aquaticus* is 2.165 nm. Contrary to EF1A from *E. coli*, the thermal stability of EF1A from *T. thermophilus* only slightly depends on the presence of GDP in the molecule. The free EF1A and EF1A·GDP from *T. thermophilus* have an almost equal rate of hydrogen/deuterium exchange (*16*).

GDP/GTP exchange changes mutual positions of the domains toward a more compact state, demonstrating the high plasticity of EF1A (*7, 8*). The two parts of the molecule, one of them corresponding to domain I and another comprising domains II and III, move toward each other as rigid bodies. Domain II moves along with domain III and forms a largely polar interface with domain I. It was shown that binding of the aminoacyl-tRNA occurs in a cleft formed between the parts of EF1A·GTP (*6*). The ternary complex consisting of yeast phenylalanyl-tRNA, *T. aquaticus* elongation factor EF1A, and GDPPNP is elongated (11.5 nm by 4.0 nm by 6.4 nm) and has an overall shape resembling a corkscrew. The theoretical radius of gyration calculated from such three-axis ellipsoid is 3.075 nm. It is assumed that interaction of EF1A·GTP with the aminoacyl-tRNA slightly compresses the protein molecule (*6, 19*).

The structure of eEF1A unlike its prokaryotic counterpart is poorly understood. The X-ray structure of the eEF1A-like elongation factor in complex with GDP from the archaeon *Sulfolobus solfataricus* (molecular mass 48.5 kDa) has been described (*20*). The structure of the complex exhibits a triangular shape with a peculiar large hole, located at one side of the molecule. The polypeptide chain (nine amino acid residues) joins domain I and domain II. This connecting peptide adopts a rather rigid structure, despite the absence of stabilizing interactions with the rest of the protein. The theoretical radius of gyration of the protein calculated with the CRYSOL program is 2.549 nm.

Recently (*21*), X-ray data have been published for the yeast eEF1A (molecular mass 50 kDa) crystallized in a complex with a fragment of the nucleotide-exchanging subunit eEF1Bα (molecular mass 11 kDa). As expected, eEF1A contains three structural domains similar to EF1A. The complex has overall dimensions of 7.6 nm by 6.7 nm by 5.2 nm. The theoretical radius of gyration calculated for this spheroid is 2.546 nm.

At present there is no information on the crystal or solution structure of mammalian eEF1A. It is not known how the conformation of eEF1A is affected by its interaction with tRNA either. To address the issues, we have analyzed here the structure of both rabbit liver eEF1A·GDP and its complex with tRNA in solution by the neutron scattering and microcalorimetry methods. We have found that rabbit liver eEF1A has a considerably more disordered conformation than its prokaryotic analogue. The conformation of eEF1A becomes significantly more compact during the interaction with tRNA. The eEF1A molecule is hypothesized to adopt an extended conformation due to the loss of the association between domains I and III. The interaction is renewed upon addition of the biological ligand (tRNA) leading to significant compactization of the protein.

EXPERIMENTAL PROCEDURES

Isolation and Characterization of eEF1A. eEF1A was purified from rabbit liver using a combination of gel filtration, ion-exchange, and hydroxyapatite chromatographies in the presence of 25% glycerol and 20 μM GDP as described previously (*22*). GDP/[^{3}H]GDP exchange in the eEF1A molecule was carried out as in ref *23*. The eEF1A ability to support the poly(U)-dependent translation in the mammalian cell-free system assembled from individual components was investigated as described (*24*).

The effect of eEF1A·GTP on the spontaneous deacylation of aminoacyl-tRNA was studied at 25 °C in 110 μL of 70 mM imidazole, pH 7.0, 50 mM NH$_4$Cl, 10 mM MgCl$_2$, 2 mM DTT, 10% glycerol, 0.2 mM GTP, and 2.7 μM [^{14}C]-Leu-tRNA^{Leu} (from beef liver). At definite time points (0, 0.5, 1, 2 and 3 h) the 20 μL aliquots were immersed into 1 mL of ice-cold 10% TCA. The mixtures were filtered through GF/C (Whatman) and washed twice with 5% cold TCA. The radioactivity of dried filters was counted using toluene-based scintillation fluid.

The concentration of eEF1A was measured by the conventional procedure (*25*) using bovine serum albumin as a standard.

Isolation of tRNA. Total tRNA was isolated from rabbit liver as described (*26*). The tRNA preparation enriched with tRNA^{Val} was purified by HPLC chromatography using an ion-exchange DEAE column (Phenomenex). tRNA^{Val} constituted about 45% of the tRNA preparation.

Isolation and Characterization of EF1A from T. thermophilus. The elongation factor EF1A purification from *T. thermophilus* was carried out as described (*27*). The crude cell-free extract was a kind gift of Dr. M. Garber (Institute of Protein Research, RAS, Pushchino). EF1A free from nucleotide was prepared as in ref *28*. The EF1A concentration was measured using a molar extinction coefficient $\epsilon_{280} = 32900$ M^{-1} cm^{-1}.

Scanning Microcalorimetry. Calorimetric measurements were done on a precision scanning microcalorimeter SCAL-1 (Scal Co. Ltd., Pushchino, Russia) with glass cells (volume 0.3 mL) at scanning rate of 1.0 K/min (*29*). Degassing during the calorimetric experiments was prevented by maintaining an additional constant pressure of 3.0 atm in the cells.

Before the measurements all samples were dialyzed overnight against the corresponding buffer. The concentration of protein used in the calorimetric experiments was in the range of 0.7−1.0 mg/mL. A typical value of 0.74 cm^3/g for the partial specific volume for globular proteins was accepted. The analyses of the heat capacity curves were undertaken using the fitting routine based on the two-state transition (*30*).

Neutron Scattering. Two neutron scattering methods were applied during this study: small angle neutron scattering (SANS) in a H$_2$O−solvent and polarization-dependent neutron scattering in a solvent containing 39% *h*-glycerol, 15% *d*-glycerol, and 0.8% Cr(V)-EHBA [sodium bis(2-ethyl-2-hydroxybutyrato)oxochromate(V) monohydrate {Na[Cr-(C$_6$H$_{10}$O$_3$)$_2$]·H$_2$O}] diluted in the deuterated D$_2$O−sample solution.

The small angle neutron scattering experiments were carried out on the SANS camera of Paul Scherrer Institute (Switzerland) at the wavelength of 0.6 nm. The quartz cuvette of 1 mm thickness was thermostated at 4 °C. The range of scattered vectors was 0.1−2.5 nm^{-1}. The raw data were corrected on the detector sensitivity and normalized to the absolute scale by using the scattering of light water at the same experimental conditions.

The stoichiometry of the [eEF1A·GDP·tRNA] complex was determined from the value of the initial ordinate $I(0)/C$ on a Guinier plot. It is known that

$$I(0)/C \sim \sum C_i M_i (v_i \Delta \rho_i)^2 / \sum C_i \qquad (1)$$

where C_i is the weight concentration of ith component, M_i is the molecular mass, v_i is the partial specific volume, and $\Delta \rho_i$ is the excess of scattering density.

For eEF1A and tRNA $v = 0.74$ cm^3/g and $v = 0.55$ cm^3/g and $\Delta \rho = 2.0 \times 10^{-14}$ cm/Å^3 and $\Delta \rho = 3.8 \times 10^{-14}$ cm/Å^3, respectively. Taking into account the high affinity of eEF1A·GDP for deacylated tRNA (*31*) and using $M_{eEF1A}/M_{tRNA} \sim 2$, one can estimate the value of $I(0)/C$ for a mixture of eEF1A and tRNA.

The polarization-dependent neutron scattering experiments were performed using the SANS-1 beam line of the GKSS Research Center as described earlier (*32*). The idea was to create contrast variation only by changing the polarization of the hydrogen atoms (spin contrast variation). This has the great advantage that systematic errors from different samples can be neglected since only one sample is needed. In principle, it should even be possible to find a matching polarization for either protein or RNA contributions of the scattering.

For the polarization-dependent measurements the sample plate was cooled to approximately 120 mK in a ^{3}He/^{4}He dilution refrigerator. Following the procedure of dynamic nuclear polarization the hydrogen (=proton) spins in the sample were aligned with respect to the external magnetic field of 2.5 T up to a maximum negative polarization, and polarization-dependent neutron scattering data were taken.

The sample with eEF1A (10 mg/mL) was measured at proton polarization $P_H = \pm60\%$, $\pm50\%$, $\pm30\%$ and in the unpolarized case giving data for seven different contrast conditions. The sample containing tRNA (2 mg/mL) was measured only at zero polarization. In the case of the [eEF1A·GDP·tRNA] complex five different contrast conditions were obtained: $P_H = 0\%$, $\pm40\%$, and $\pm28\%$. In all
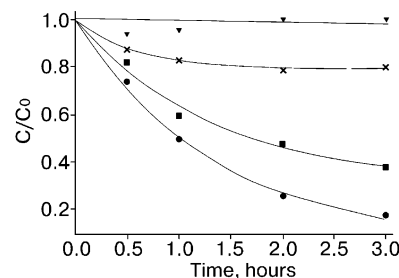

FIGURE 1: Influence of eEF1A·GTP on spontaneous hydrolysis of [^{14}C]Leu-tRNA^{Leu}. 2.7 μM [^{14}C]Leu-tRNA^{Leu} was incubated alone (●) and in the presence of 2 μM (■), 4.5 μM (×), and 6 μM (▼) eEF1A·GTP. Incubation was carried out at 25 °C in the buffer containing 0.2 mM GTP and 10% glycerol. C/C_0 is the fraction of unhydrolyzed [^{14}C]Leu-tRNA^{Leu}.

cases the data were taken at three different distances with 0.85 nm neutrons.

RESULTS

Functional Tests of Mammalian eEF1A. To make sure that the eEF1A preparation was fully active and could be adequately used for physical studies, different functional characteristics of the protein were investigated.

Practically all molecules of eEF1A after purification contained endogenous GDP as determined by HPLC chromatography (*22*). In the GDP/[^{3}H]GDP exchange test more than 95% of eEF1A·GDP molecules were capable to exchange endogenous GDP for [^{3}H]GDP. Importantly, GDP-exchanging properties of eEF1A were similar before and after the neutron scattering experiments.

The ability of rabbit eEF1A used in this study to interact with aminoacyl-tRNA and GTP resulting in a ternary complex formation was demonstrated in the experiment where aminoacyl-tRNA was protected from spontaneous deacylation in the presence of eEF1A·GTP (Figure 1). Total protection during 3 h was achieved at the aminoacyl-tRNA: eEF1A ratio of 1:2, suggesting a rather high ability of eEF1A to interact with aminoacyl-tRNA. High functional activity of eEF1A was also demonstrated in the experiments on the stimulation of aminoacyl-tRNA binding to the ribosomal A-site and poly(U) translation in a cell-free protein synthesizing system assembled from individual components [40S and 60S ribosomal subunits, [^{14}C]Phe-tRNA, eEF2, poly(U) (Figure 2)].

Thus, we concluded that the eEF1A preparation was functionally active.

Scanning Microcalorimetry of eEF1A. Figure 3 shows the temperature dependence of the excess heat capacity of eEF1A (a) and EF1A (b) measured in the absence of GDP (see Experimental Procedures). The heat absorption curves for both proteins reveal a complex shape which correlates with recently published thermodynamic data for EF1A obtained under somewhat different buffer conditions (*33*). The excess heat capacity curves were deconvoluted into three peaks using the best fit program (*30*) with each peak corresponding to two-state transition; i.e., the denaturation enthalpy calculated from the calorimetric curve (ΔH_{cal}) coincided with the effective van't Hoff enthalpy (ΔH_{eff}). It implies that each of proteins consists of three cooperative thermodynamic domains with the appropriate transition temperatures. The thermodynamic parameters characterizing these transitions
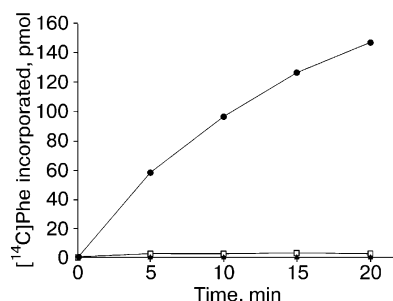
FIGURE 2: Dependence of the poly(U)-directed poly(Phe) synthesis on factor addition: (▲) factor-free translation; (□) translation in the presence of eEF2 only; (●) translation in the presence of eEF1A and eEF2. The reaction was carried out in 100 μL of reaction mixture containing 5 mM MgCl$_2$, 100 mM NH$_4$Cl, 3.5 mM spermidine, 0.4 mM GTP, 1 mM ATP, 18 pmol of 80S ribosomes, 15 μg of poly(U), 20 pmol of eEF2, and 50 pmol of eEF1A. No aminoacyl-tRNA was added, but instead 700 pmol of tRNA^{Phe} was preincubated with 30 ng of PheRS, 3 mM ATP, and 60 μM [^{14}C]Phe for 10 min at 37 °C.
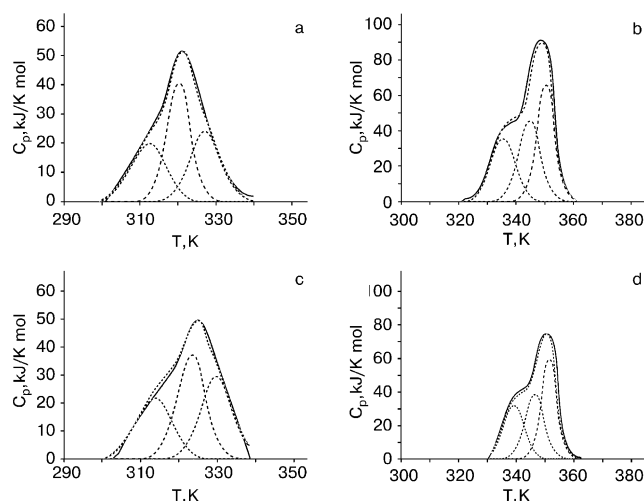

FIGURE 3: Temperature dependence of the excess heat capacity of eEF1A (a) and EF1A (b) in 20 mM Tris-HCl, pH 7.9, 10 mM magnesium acetate, and 5 mM 2-mercaptoethanol; eEF1A (c) and EF1A (d) in the same buffer with 20 μM GDP. Solid line: experimental curve. Dotted line: calculated heat capacity function.

are given in Table 1. It should be noted that the presence of three thermodynamic domains in the mammalian protein molecule correlates with the fact that both prokaryotic and lower eukaryotic proteins have three structural domains revealed by X-ray analysis (see the introduction).

In the buffer containing 20 μM GDP (Figure 3c,d), the heat absorption curves for each protein can also be deconvoluted into three heat absorption peaks. The melting of all three domains occurs at the higher temperatures (see Table 1). Noteworthy, the principal character of the protein melting is not changed within the GDP concentration range from 20 to 200 μM (Tiktopulo et al., unpublished).

The heat effect (heat absorption during the denaturation process) differs considerably for the two proteins. While for the prokaryotic protein the transition enthalpy of all three domains corresponds to the melting of small compact globular proteins with a specific heat of denaturation of 7 cal/g, this value for the eukaryotic protein is much lower (about 4 cal/g). Strictly speaking, these values should be compared at the same temperature. According to Kirchhoff's

equation the temperature dependence of the denaturation enthalpy can be described as

$$\Delta H_t = \Delta H_d - \Delta C_p(T_d - T_t) \qquad (2)$$

where ΔH_d is the enthalpy of denaturation at temperature T_d, ΔH_t is the enthalpy of denaturation at temperature T_t, and ΔC_p is the heat capacity jump during the heat transition.

In our experiments the heat capacity jump for the eukaryotic protein was very small. Hence, the enthalpy of denaturation only slightly depends on temperature, at least at the first approximation. Thus, the difference in specific enthalpy values for the two proteins does exist, and the eEF1A molecule (or its part) has a far more disordered conformation than its prokaryotic analogue. The GDP effect on the melting curves of EF1A and eEF1A is different. In the case of EF1A the addition of 20 μM GDP causes the significant increase of the enthalpy values of the first two peaks whereas for eEF1A one can observe the preferable increase of the third peak stability (see Table 1).

Neutron Scattering of eEF1A. Figure 4 shows the dependence of the neutron scattering intensity I on the scattering vector Q ($Q = 4\pi \sin(\Theta)/\lambda$, where λ is the wavelength of incident neutrons and 2Θ is the scattering angle) in Guinier coordinates (log I vs Q^2) extrapolated to the zero concentration of eEF1A·GDP.

The protein molecular mass calculated from the scattering intensity value extrapolated to the zero scattering angle [$I(0)/C$] is 48.6 ± 2.0 kDa, which is close to 50.34 kDa calculated from the primary sequence (*34*). The correspondence of the slope obtained to the correct molecular mass indicates that there is no aggregation of eEF1A·GDP molecules despite the high concentrations (40−120 μM) of the protein in these experiments. The partial specific volume calculated from amino acid composition (*35*) is equal to 0.74 cm^3/g. The values of gyration radii calculated from the Guinier graph do not depend on the concentration. The average value of a gyration radius was 5.2 ± 0.2 nm, evidencing an extremely extended conformation of protein eEF1A in solution at 20 μM GDP.

eEF1A·GDP was studied independently by spin-dependent neutron scattering in the presence of 10 μM GDP. The scattering intensity of negative hydrogen polarization decreased linearly with the decrease of spin polarization to zero polarization. The curves were very similar; only very close to the matching polarization the shape changed. From all curves (negative or zero polarization values) the radius of gyration found was 6.1 ± 0.5 nm. Since the statistical errors for positive polarization were very high, we did not take correspondent data into account. An extrapolation to zero contrast was not made in this case but will be of interest for further exploitation of the method of spin contrast variation. A direct comparison of the scattering curves at low temperatures with measurements at room temperature was not made since it is well established for ribosome (*36, 37, 38*) and chaperone (R. Willumeit, personal communications) samples that the freezing process does not influence the shape of the molecules.

Neutron Scattering of the [eEF1A·GDP·tRNA] Complex. The formation of the [eEF1A·GDP·tRNA] complex was studied by small angle neutron scattering at different molar eEF1A:tRNA ratios (1:2, 1:3, 2:1, 3:1). Figure 5 shows

Table 1: Thermodynamic Parameters Describing the Melting of eEF1A and EF1A

protein	$q,^a$ cal/g	$\Delta H_{cal},^a$ kJ/mol	$\Delta H_1,^a$ kJ/mol	$\Delta H_2,^a$ kJ/mol	$\Delta H_3,^a$ kJ/mol	$T_{d1},^a$ K	$T_{d2},^a$ K	$T_{d3},^a$ K
eEF1A	4.30	905.0	256.0	361.0	288.0	311.7	320.1	326.9
eEF1A + 20 μM GDP	4.40	931.0	238.0	363.0	330.0	312.9	322.0	330.1
EF1A	6.60	1192.0	340.5	370.0	481.5	335.8	344.3	350.1
EF1A + 20 μM GDP	6.95	1252.0	361.0	398.0	493.2	339.1	347.4	352.0

^{a} q is the specific heat of denaturation; calorimetric enthalpy $\Delta H_{cal} = Mq$, where M is the molecular mass; ΔH_i and T_{di} are the calorimetric enthalpy and midpoint temperature of each heat transition peak, correspondingly.
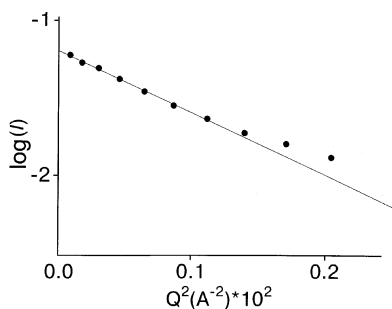

FIGURE 4: Dependence of neutron scattering intensity I on scattering vector Q in Guinier coordinates ($\log I$ vs Q^2) extrapolated to the zero concentration of eEF1A at 20 μM GDP.
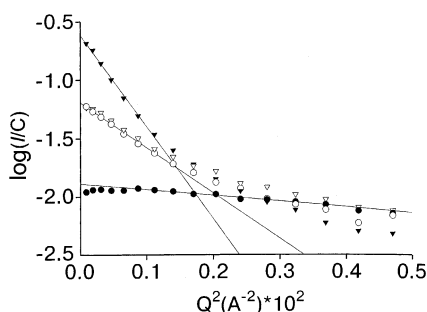

FIGURE 5: Dependence of neutron scattering intensity I on scattering vector Q in Guinier coordinates to tRNA ($\bullet$), eEF1A ($\circ$), eEF1A: tRNA = 1:3 ($\triangledown$), and eEF1A:tRNA=3:1 ($\blacktriangledown$).

Guinier dependencies of the neutron scattering intensity normalized for the concentration at the molar eEF1A:tRNA ratios of 1:3 and 3:1. The essential changes of $I(0)/C$ were observed at the excess of protein over tRNA. From the intercept value $I(0)/C$ the approximate stoichiometry of the complex was estimated as described in Experimental Procedures. Preliminary interpretation of the data could be that the complex consists of two protein molecules and one tRNA molecule. However, further investigations with another methodical approach may be useful to clarify the point more definitely.

In Figure 6 the scattering curves obtained in a wide range of scattering vectors (from 0.1 to 1.5 nm^{-1}) are plotted in Kratky coordinates (IQ^2 vs Q). In that case the scattering curve for eEF1A is typical for nonglobular disordered structures (*39*). Such shape of curves was observed also for the protein:tRNA mixtures at ratios of 1:3 and 1:2 (data are not shown for the sake of clarity of the picture). On the contrary, the scattering curves became much closer to those typical for globular structures (*39*) when eEF1A:tRNA ratios were 3:1 and 2:1 (Figure 6; data at 2:1 ratio are not shown for the sake of clarity of the picture). Thus, the formation of the [eEF1A·GDP·tRNA] complex led to the essential compactization of the eEF1A molecule.
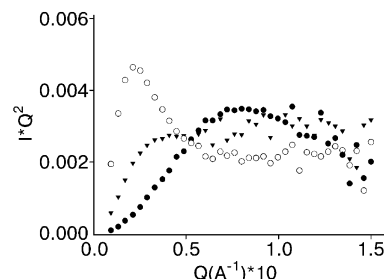

FIGURE 6: Dependence of neutron scattering intensity I on scattering vector Q in Kratky coordinates for tRNA ($\bullet$), eEF1A ($\blacktriangledown$), and eEF1A:tRNA = 3:1 ($\circ$).

DISCUSSION

The Mammalian Translation Factor Has Significantly More Extended Conformation in Solution than the Prokaryotic Analogue. According to the neutron scattering measurements the rabbit liver eEF1A in the presence of 20 μM GDP has a radius of gyration of 5.2 ± 0.2 nm, which is 2-fold more than the calculated radius of gyration of its bacterial analogue EF1A (2.6 nm, taking into account the molecular mass difference; see the introduction). Thus, eEF1A is more extended in solution than EF1A. According to the scanning microcalorimetry the eEF1A molecule contains elements of tertiary structure (three thermodynamic domains), melting of which is reflected by the curves of heat absorption. The positions of the peaks are affected by GDP. The characteristic feature of the eEF1A melting was that the heat effect is much lower than that expected for globular proteins with inflexible three-dimensional structure. Such a behavior was observed in a limited set of proteins containing unstructured regions (histones, ribosomal protein L7) (*40*).

Thus, both the neutron scattering and microcalorimetry data evidence the existence of a significantly disordered structure of the mammalian eEF1A in solution. The following possible structure of the mammalian eEF1A in solution could be proposed. The eEF1A molecule consists of three distinct globular domains, connected by rigid interconnecting peptides, like prokaryotic EF1A. For *S. solfataricus* eEF1A (*20*) a large interface between domains I and III is shown to be responsible for the protein heat stability. Therefore, domains I and III of the mammalian protein are hypothesized to be disconnected in solution, resulting in the decreased heat stability of eEF1A in comparison with the bacterial analogue. Taking the length of the polypeptide chain joining domain I and domain II equal to 1.5 nm, the length of polypeptide chain joining domain II and domain III equal to 1.0 nm (*13*), and approximating each domain by sphere with radius of 2.1 nm, one can calculate the radius of gyration of such a trumbell model. This value is about 5.0 nm, which is close to our experimental data obtained by the neutron scattering.

Such an "open" conformation of eEF1A may explain why high glycerol concentration is absolutely required for isolation and preservation of activity of the mammalian protein contrary to the bacterial EF1A (*23*, *41*). Glycerol seems to stabilize the conformation of the mammalian elongation factor.

Peculiarities of Formation of the Noncanonical [eEF1A·GDP·tRNA] Complex. eEF1A·GDP is known to bind uncharged tRNA (*5*). This binding is thought to be rather specific since the regions of tRNA protected by eEF1A·GDP from nuclease hydrolysis and chemical modifications in footprinting assay closely resemble those of aminoacyl-tRNA involved in the interaction with EF1A·GTP according to the X-ray studies (*6*). The [eEF1A·GDP·tRNA] complex is thermodynamically stable [K_d is 20 nM as determined by the fluorescence polarization studies (*31*)].

The neutron scattering data presented on the Kratky plot (Figure 6) and the value of the eEF1A radius of gyration (about 3.2 nm) inside the [eEF1A·GDP·tRNA] complex measured by polarization-dependent neutron scattering (Willumeit et al., to be published) show essential compactization of the protein molecule upon complex formation. The stoichiometry of the [eEF1A·GDP·tRNA] complex appears to be two molecules of the protein per one molecule of tRNA. The stoichiometry of the regular ternary prokaryotic complex [EF1A·GTP·aminoacyl-tRNA] was not determined unambiguously. One set of data demonstrated that the complex might include one molecule of tRNA and two molecules of the protein, depending on the experimental conditions (*42*, *43*), while other experiments showed the stoichiometry of the protein and tRNA in the ternary complex being 1:1 (*19*, *44*). The crystallographic data describing the [EF1A·GDPPNP·aminoacyl-tRNA] complex favored the last point of view, though the crystallization conditions were far from the physiological conditions (*6*). The neutron scattering experiments presented in this paper suggest that in the higher eukaryotes the stoichiometry of 2:1 for the factor−tRNA binding might be also found at least in the [eEF1A·GDP·tRNA] complex. The biological importance of the presence of two protein molecules and one tRNA molecule in the complex remains unclear though such a stoichiometry in the classical ternary complex is suggested to support the translation accuracy under some conditions (*43*).

Functioning of the Elongation Factors 1A in the Prokaryotic and Eukaryotic Protein Synthesis. What could be the biological sense of the partially unfolded conformation of the mammalian eEF1A in solution? Structural aspects of the functioning of the translation machinery in prokaryotes and higher eukaryotes do not appear to be identical. The mammalian protein synthesizing apparatus is highly compartmentalized, which is proven now both in vitro (*2*), and in vivo (*45*, *46*). The prokaryotic factor EF1A·GTP has in solution the compact conformation which is not changed much upon interaction with aminoacyl-tRNA (*19*). On the contrary, mammalian eEF1A has in solution a significantly extended conformation, which undergoes dramatic changes during its interaction with tRNA. That might be a reason for observed significant difficulties in the crystallization of the isolated higher eukaryotic factor 1A (unpublished observation).

Thus, the idea of the absolute similarity of the functioning of the elongation factors 1A in prokaryotic and eukaryotic translation may be reconsidered with more critical view. The concept of the "conformational switch" between functional GTP and nonfunctional GDP conformations of the prokaryotic EF1A which sharply alter the protein affinity for such partners as tRNA and ribosome might not be plainly applicable for the mammalian protein because of a possibly less pronounced difference between GDP and GTP solution conformations of eEF1A (*1*). However, significant conformational changes in the eEF1A molecule do occur depending on whether the factor is alone or interacting with some of its biological partners. Such way of functioning may be optimal under the conditions of compartmentalized and channeled mammalian protein synthesis. Therefore, the comparison of the eEF1A conformations during the interaction with deacylated and aminoacyl-tRNA, with aminoacyl-tRNA synthetase and 80S ribosome, will be of special interest for future investigations.

The Mammalian Translation Elongation Factor 1A as a Possible Member of the Family of Unstructured Proteins. It has long been axiomatic that the majority of the biological functions in the cell (such as enzymatic catalysis, immunological and receptor recognition) are performed by proteins with unique three-dimensional structure. However, there is an increasing set of data concerning proteins that are totally or partially unstructured under physiological conditions and yet are functional. Intrinsically disordered proteins adopt folded structures upon binding to their biological ligands. The characteristic features of those proteins are the high positive charge of a molecule and participation in the most important regulatory functions in the cell (*47*). Some translational components belong to this family. For example, the 98 amino acid long domain of the eukaryotic translation initiation factor eIF4G is disordered but becomes structured upon the interaction with initiation factor eIF4E (*48*).

The experimental data presented here give the basis to conclude that eEF1A, which is highly positively charged (p*I* 9.1), may be partially unstructured in solution and, thus, can be a member of the family of unstructured proteins. The chaperone properties of eEF1A (those are also characteristic for such polypeptides) have been recently found as well (*49*; Turkovskaya et al., in press). We believe that the partially unstructured solution conformation of eEF1A might explain the well-known ability of the protein to form a complex with very different ligands such as actin (*50*), tubulin (*51*), calmodulin (*52*), calmodulin-dependent protein kinase (*53*), some regulatory proteins (*54*, *55*), the components of the ubiquitin-dependent proteolytic system (*56*), and viral RNA (*57*). Taking into account the abundant quantity of eEF1A in the cell, the eEF1A−ligand interaction in cytoplasm may be called "net-casting" by analogy with the recently proposed "fly-casting" (*58*) mechanism for the interaction of unstructured regulatory proteins and their targets present in cells at low concentrations.

REFERENCES

1. Negrutskii, B. S., and El'skaya, A. V. (1998) Eukaryotic translation elongation factor 1α: Structure, expression, functions, and possible role in aminoacyl-tRNA channeling, *Prog. Nucleic Acids Res. Mol. Biol. 60*, 47−78.

2. Ryazanov, A. G., Ovchinnikov, L. P., and Spirin, A. S. (1987) Development of structural organization of protein-synthesizing machinery from prokaryotes to eukaryotes, *Biosystems 20*, 275−288.

3. Negrutskii, B. S., Stapulionis, R., and Deutscher, M. P. (1994) Supramolecular organization of the mammalian translation system, *Proc. Natl. Acad. Sci. U.S.A. 91*, 964−968.

4. Negrutskii, B. S., and Deutscher, M. P. (1991) Channeling of aminoacyl-tRNA for protein synthesis *in vivo*, *Proc. Natl. Acad. Sci. U.S.A. 88*, 4991−4995.

5. Petrushenko, Z. M., Negrutskii, B. S., Ladokhin, A. S., Budkevich, T. V., Shalak, V. F., and El'skaya, A. V. (1997) Evidence for the formation of an unusual ternary complex of rabbit liver tRNA with GDP and deacylated tRNA, *FEBS Lett. 407*, 13−17.

6. Nissen, P., Kjeldgaard, M., Thirup, S., Polekhina, G., Reshetnikova, L., Clark, B. F. C., and Nyborg, J. (1995) Crystal structure of the ternary complex of Phe-tRNA^Phe, EF-Tu, and a GTP analog, *Science 270*, 1464−1472.

7. Kjeldgaard, M., Nissen, P., Thirup, S., and Nyborg, J. (1993) The crystal structure of elongation factor EF-Tu from *Thermus aquaticus* in the GTP conformation, *Structure 1*, 35−50.

8. Berchtold, H., Reshetnikova, L., Reiser, C. O., Schirmer, N. K., Sprinzl, M., and Hilgenfeld, R. (1993) Crystal structure of active elongation factor Tu reveals major domain rearrangements, *Nature 365*, 126−132.

9. Kawashima, G., Berthet-Colominas, C., Wulff, M., Cussack, S., and Leberman, R. (1996) The structure of the *Echerichia coli* EF-Tu:EF-Ts complex at 2.5 Å resolution, *Nature 379*, 579−518.

10. Polekhina, G., Thirup, S., Kjeldgaard, M., Nissen, P., Lippman, C., and Nyborg, J. (1996) Helix unwinding in the effector region of elongation factor EF-Tu·GDP, *Structure 4*, 1141−1151.

11. Song, H., Parsons, M. R., Rowsell, S., Leonard, G., and Phillips, S. E. (1999) Crystal structure of intact elongation factor EF-Tu from *Escherichia coli* in GDP conformation at 2.05 Å resolution, *J. Mol. Biol. 285*, 1245−1256.

12. Cavallius, J., and Merrick, W. C. (1992) Nucleotide sequence of rabbit elongation factor 1α cDNA, *Nucleic Acids Res. 20*, 1422−1445.

13. Kjeldgaard, M., and Nyborg, J. (1992) Refined structure of elongation factor EF-Tu from *Escherichia coli*, *J. Mol. Biol. 223*, 721−742.

14. Svergun, D., Barberato, C., and Koch, M. H. J. (1995) CRYSOL−a program to evaluate X-ray solution scattering of biological macromolecules from atomic coordinates, *J. Appl. Crystallogr. 28*, 768−773.

15. Serdyuk, I. N., Pavlov, M. Yu., Rublevskaya, I. N., Zaccai, G., and Leberman, R. (1994) The triple isotopic substitution method in small angle neutron scattering. Application to the study of the ternary complex EF-Tu·GTP·aminoacyl-tRNA, *Biophys. Chem. 53*, 123−130.

16. Ohta, S., Nakanishi, M., Tsuboi, M., Arai, K., and Kaziro, Y. (1977) Structural fluctuation of the polypeptide-chain elongation factor Tu, *Eur. J. Biochem. 78*, 599−608.

17. Kushiro, M., Shimizu, M., and Tomita, K. (1987) Molecular cloning and sequence determination of the tuf gene coding for the elongation factor Tu of *Thermus thermophilus* HB8, *Eur. J. Biochem. 170*, 93−98.

18. Voss, R. H., Hartmann, R. K., Lippmann, C., Alexander, C., Jahn, O., and Erdmann, V. (1992) Sequence of the tufA gene encoding elongation factor EF-Tu from *Thermus aquaticus* and overproduction of the protein in *Escherichia coli*, *Eur. J. Biochem. 207*, 839−846.

19. Bilgin, N., Ehrenberg, M., Ebel, C., Zaccai, G., Sayers, Z., Koch, M. H. J., Svergun, D. I., Barberato, C., Volkov, V., Nissen, P., and Nyborg, J. (1998) Solution structure of the ternary complex between aminoacyl-tRNA, elongation factor Tu and guanosine triphosphate, *Biochemistry 37*, 8163−8172.

20. Vitagliano, L., Masullo, M., Sica, F., Zagari, A., and Bocchini, V. (2001) The crystal structure of *Sulfolobus solfataricus* elongation factor 1α in complex with GDP reveals novel feature in nucleotide binding and exchange, *EMBO J. 20*, 5305−5311.

21. Andersen, G. R., Pedersen, L., Valente, L., Chatterjee, I., Kinzy, T. G., Kjeldgaard, M., and Nyborg, J. (2000) Structural basis for nucleotide exchange and competition with tRNA in the yeast elongation factor complex eEF1A:eEF1Bα, *Mol. Cell 6*, 1261−1266.

22. Shalak, V. F., Budkevich, T. V., Negrutskii, B. S., and El'skaya, A. V. (1997) A fast and effective method for purification of elongation factor 1α from rabbit liver, *Ukr. Biokhim. Zh. 69*, 104−109.

23. Carvalho, M. D., Carvalho, J. F., and Merrick, W. C. (1984) Biological characterization of various forms of elongation factor 1 from rabbit reticulocytes, *Arch. Biochem. Biophys. 234*, 603−611.

24. El'skaya, A. V., Ovcharenko, G. V., Pal'chevskii, S. S., Petrushenko, Z. M., Triana-Alonso, F. J., and Nierhaus, K. H. (1997) Three tRNA binding sites in rabbit liver ribosomes and role of the intrinsic ATPase in 80S ribosomes from higher eukaryotes, *Biochemistry 36*, 10492−10497.

25. Bradford, M. M. (1976) A rapid and sensitive method for the quantitation of microgram quantities of protein utilizing the principle of protein-dye binding, *Anal. Biochem. 72*, 248−254.

26. El'skaya, A. V., and Negrutskii, B. S. (1987) The interaction between biologically inactive tRNA conformers and leucyl-tRNA synthetase from rabbit liver, *Eur. J. Biochem. 164*, 65−69.

27. Arai, O., Ota, Y., Arai, N., Nakamura, S., Henneke, C., Oshima, T., and Kaziro, Y. (1978) Studies on polypeptide-chain-elongation factors from an extreme thermophile, *Thermus thermophilus* HB8, *Eur. J. Biochem. 92*, 509−519.

28. Limmer, S., Reiser, C. O. A., Schirmer, N. K., Grillenbeck, N. W., and Sprinzl, M. (1992) Nucleotide binding and GTP hydrolysis by elongation factor Tu from *Thermus thermophilus* as monitored by proton NMR, *Biochemistry 31*, 2970−2977.

29. Senin, A. A., Potekhin, S. A., Tiktopulo, E. I., and Filimonov, V. V. (2000) Differential scanning microcalorimeter Scal-1, *J. Therm. Anal. Calorim. 62*, 153−160.

30. Privalov, P. L., and Potekhin, S. A. (1986) Scanning microcalorimetry in studying temperature-induced changes in proteins, *Methods Enzymol. 131*, 1−51.

31. Petrushenko, Z. M., Budkevich, T. V., Shalak, V. F., Negrutskii, B. S., and El'skaya A. V. (2002) Novel complexes of mammalian translation elongation factor eEF1A·GDP with uncharged tRNA and aminoacyl-tRNA synthetase. Implications for tRNA channeling, *Eur. J. Biochem. 269*, 4811−4818.

32. Zhao, J., and Stuhrmann, H. B. (1993) The in situ structure of the L3 and L4 proteins of the large subunit of *E. coli* ribosomes as determined by nuclear-spin contrast variation, *J. Phys. 3*, 233−236.

33. Seldak, E., Sprinzl, M., Grillenbeck, N., and Antalik M. (2002) Microcalorimetric study of elongation factor Tu from *Thermus thermophilus* in nucleotide-free, GDP and GTP forms and in the presence of elongation factor Ts, *Biochim. Biophys. Acta 1596*, 357−365.

34. Rosenberry, T. L., Krall, J. A., Dever, T. E., Haas, R., Louvard, D., and Merrick, W. C. (1989) Biosynthetic incorporation of [^3H]-ethanolamine into protein synthesis elongation factor 1α reveals a new posttranslational protein modification, *J. Biol. Chem. 264*, 7096−7099.

35. Zamyatnin, A. A. (1984) Amino acid, peptide and protein volume in solution, *Annu. Rev. Biophys. Bioeng. 13*, 145−165.

36. Burkhardt, N., Diedrich, G., Nierhaus, K. H., Meerwinck, W., Stuhrmann, H. B., Pedersen, J. S., Koch, M. H. J., Volkov, V. V., Kozin, M. B., and Svergun, D. I. (1997) Architecture of the *E. coli* 70S ribosomes, *Phys. B 234*, 199−201.

37. Svergun, D. I., Burkhardt, N., Pedersen, J. S., Koch, M. H. J., Volkov, V. V., Kozin, M. B., Meerwinck, W., Stuhrmann, H. B., Diedrich, G., and Nierhaus, K. H. (1997a) Solution scattering structural analysis of the 70S *Escherichia coli* ribosome by contrast variation. I. Invariants and validation of electron microscopy models, *J. Mol. Biol. 271*, 588−601.

38. Svergun, D. I., Burkhardt, N., Pedersen, J. S., Koch, M. H. J., Volkov, V. V., Kozin, M. B., Meerwinck, W., Stuhrmann, H. B., Diedrich, G., and Nierhaus, K. H. (1997b) Solution scattering structural analysis of the 70S *Escherichia coli* ribosome by contrast variation. II. A model of the ribosome and its RNA at 3.5 nm resolution, *J. Mol. Biol. 271*, 602−618.

39. Glatter, O., and Kratky, O. (1982) in *Small-angle X-ray scattering*, pp 167−196, Academic Press, London.

40. Gudkov, A. T., and Khechinashvili, N. N. (1978) Studies on the structure of protein L7/L12 from *Escherichia coli* ribosomes, *Eur. J. Biochem. 90*, 313−318.

41. Nagata, S., Iwasaki, K., and Kaziro, Y. (1976) Interaction of the low molecular weight form of elongation factor 1 with guanine nucleotides and aminoacyl-tRNA, *Arch. Biochem. Biophys. 172*, 168−177.

42. Ehrenberg, M., Rojas, A. M., Weiser, J., and Kurland, C. G. (1990) How many EF-Tu molecules participate in aminoacyl-tRNA binding and peptide bond formation in *Escherichia coli* translation?, *J. Mol. Biol. 211*, 739−749.

43. Rodnina, M. V., and Wintermeyer, W. (1995) GTP consumption of elongation factor Tu during translation of heteropolymeric mRNAs, *Proc. Natl. Acad. Sci. U.S.A. 92*, 1945−1949.

44. Bensch, K., Pieper, U., Ott, G., Schirmer, N., Sprinzl, M., and Pingoud, A. (1991) How many EF-Tu molecules participate in aminoacyl-tRNA binding?, *Biochimie 73*, 1045−1050.

45. Stapulionis, R., and Deutscher, M. P. (1995) A channeled tRNA cycle during mammalian protein synthesis, *Proc. Natl. Acad. Sci. U.S.A. 92*, 7158−7161.

46. Job, C., and Eberwine, J. (2001) Identification of sites for exponential translation in living dendrites, *Proc. Natl. Acad. Sci. U.S.A. 98*, 13037−13042.

47. Wright, P. E., and Dyson, H. J. (1999) Intrinsically unstructured proteins: reassessing the protein structure−function paradigm, *J. Mol. Biol. 293*, 321−331.

48. Hershey, P. E., McWhirter, S. M., Gross, J. D., Wagner, G., Alber, T., and Sachs, A. B. (1999) The Cap-binding protein eIF4E promotes folding of a functional domain of yeast translation initiation factor eIF4G1, *J. Biol. Chem. 274*, 21297−21304.

49. Hotokezaka, Y., Tobben, U., Hotokezaka, H., Van Leyen, K., Beatrix, B., Smith, D. H., Nakamura, T., and Wiedmann, M. (2002) Interaction of the eukaryotic elongation factor 1A with newly synthesized polypeptides, *J. Biol. Chem. 277*, 18545−18551.

50. Liu, G., Tang, J., Edmonds, B. T., Murray, J., Levin, S., and Condeelis, J. (1996) F-actin sequesters elongation factor 1α from interaction with aminoacyl-tRNA in a pH-dependent reaction, *J. Cell Biol. 135*, 953−963.

51. Moore, R. C., and Cyr, R. J. (2000) Association between elongation factor-1α and microtubules in vivo is domain dependent and conditional, *Cell Motil. Cytoskeleton 45*, 279−292.

52. Kaur, K. J., and Ruben, L. (1994) Protein translation elongation factor-1α from *Trypanosoma brucei* binds calmodulin, *J. Biol. Chem. 269*, 23045−23050.

53. Wang, W., and Poovaiah, B. W. (1999) Interaction of plant chimeric calcium/calmodulin-dependent protein kinase with a homolog of eukaryotic elongation factor-1α,. *J. Biol. Chem. 274*, 12001−12008.

54. Gangwani, L., Mikrut, M., Galcheva-Gargova, Z., and Davis, R. J. (1998) Interaction of ZPR1 with translation elongation factor-1α in proliferating cells, *J. Cell Biol. 143*, 1471−1484.

55. Kim, M. J., Si, F., Kim, S. J., Hong, S. B., Hwang, J. I., Lee, H. J., Lee, S. J., Chang, J. S., Lee, Y. H., Ryu, S. H., and Suh, P. G. (1999) The SH2-SH2-SH3 domain of phospholipase C-γ1 directly binds to translational elongation factor-1α, *Mol. Cells 9*, 631−637.

56. Gonen, H., Smith, C. E., Siegel, N. R., Kahana, C., Merrick, W. C., Chakraburetty, K., Schwartz, A. L., and Ciechanover, A. (1994) Protein synthesis elongation factor EF-1α is essential for ubiquitin-dependent degradation of certain Nα-acetylated proteins and may be substituted for by the bacterial elongation factor EF-Tu, *Proc. Natl. Acad. Sci. U.S.A. 91*, 7648−7652.

57. Blackwell, J. L., and Brinton, M. A. (1997) Translation elongation factor-1α interacts with the 3′ stem-loop region of West Nile virus genomic RNA, *J. Virol. 71*, 6433−6444.

58. Dyson, H. J., and Wright, P. E. (2002) Coupling of folding and binding for unstructured proteins, *Curr. Opin. Struct. Biol. 12*, 54−60.